Low-frequency Raman scattering of liquid CCl 4 , CHCl 3 , and acetone

Yuko Amo and Yasunori Tominaga

Citation: The Journal of Chemical Physics **109**, 3994 (1998); doi: 10.1063/1.476999
View online: http://dx.doi.org/10.1063/1.476999
View Table of Contents: http://scitation.aip.org/content/aip/journal/jcp/109/10?ver=pdfcov
Published by the AIP Publishing

Low-frequency Raman scattering of liquid CCl_4, $CHCl_3$, and acetone

Yuko Amo
Division of Advanced Technology for Medical Imaging, National Institute of Radiological Sciences, 9-1, Anagawa-4-chome, Inage-ku, Chiba-shi, 263 Japan

Yasunori Tominaga
Graduate School of Humanities and Sciences, Ochanomizu University, Otsuka, Bunkyo-ku, Tokyo 112-8610, Japan

(Received 5 January 1998; accepted 5 June 1998)

We report herein depolarized low-frequency Raman scattering measurements of liquid CCl_4, $CHCl_3$ and acetone. The reduced Raman spectra were analyzed for the first time using a relaxation function based on the multiple random telegraph (MRT) model of dielectric relaxation which takes into account inertia and memory effects. The imaginary part of the dielectric function of the MRT model reproduces the spectral profile of the low-frequency region of the reduced Raman spectra quite well. This indicates that the origin of the complicated central component of Raman spectra of liquids can be explained by intermolecular dynamics based on the MRT model. © *1998 American Institute of Physics.* [S0021-9606(98)51234-2]

I. INTRODUCTION

Low-frequency Raman scattering is one of the most useful methods for investigating the collective intermolecular dynamics of molecules in liquids.

Recently, the low-frequency Raman scattering of water and aqueous solutions has been analyzed using a superposition of two damped oscillator modes and one relaxation mode.[1–3] Damped oscillator modes around 180 cm^{-1} and 70 cm^{-1} were assigned to the stretching-like and bending-like vibrations, respectively. These modes are based on a tetrahedral-like cluster which consists of five water molecules. The low frequency central component below 10 cm^{-1} was fitted well by the Cole-Cole relaxation function. The origin of this relaxation mode is thought to be the making and breaking of the hydrogen bonding network in liquid water.

Optical heterodyne detected optical Raman-induced Kerr effect (OHD-RIKES) can also provide information about intermolecular and intramolecular dynamics. This method can observe spectral densities from 0 cm^{-1} to about 600 cm^{-1} in the frequency domain. Using a multimode Brownian oscillator model, the total spectrum is interpreted as superposition of linear and quadratic coupling terms.[4,5]

Terahertz time domain spectroscopy (THz TDS) can determine the frequency-dependent dielectric relaxation in the frequency range from 0.1 to 2 THz (corresponding to 3 to 60 cm^{-1}). Water and some molecular liquids have been measured by both reflection and transmission methods.[6–8] The truncated sum of Mori's continued fraction was used in the analysis of some spectra,[6,7] and multiple Debye type relaxation has also been used.[8,9]

Frequency dependent polarizability (first order susceptibility) is obtained using THz TDS, while the second order susceptibility is obtained using low-frequency Raman scattering. Low frequency Raman scattering and THz TDS experiments provide different kinds of information on the collective motion of liquids.

In liquid water and aqueous solutions, the Debye or Cole-Cole relaxation functions can be used to model the central component of Raman spectra which show a high background which extends to the high frequency region. However, these types of relaxation functions cannot be applied to simple molecular liquids because the spectra has low backgrounds in the high frequency region.

In the present paper, we propose using the imaginary part of the random telegraph model[10] of dielectric relaxation as a fitting function for the Raman susceptibility of CCl_4, $CHCl_3$ and acetone.

II. EXPERIMENT

CCl_4, $CHCl_3$ and acetone were purchased from Wako Pure Chemical Industries, Co. Ltd. Fused silica cells were used for measurements. Raman spectra were obtained using a double grating spectrometer (Ramanor U1000, Jovin-Yvon). The exciting light source was an argon ion laser (GLS2165, NEC) operating at 488 nm with power of 300 mW (for CCl_4) or 400 mW (for $CHCl_3$, acetone). Right angle scattering geometry was adopted with the (VH) configuration. The depolarized Raman spectra were recorded in the frequency region of 0 to 1000 cm^{-1} for CCl_4 and 0 to 2000 cm^{-1} for $CHCl_3$ and acetone. The spectral resolution was 1.0 cm^{-1}. All spectra were recorded at room temperature.

III. RESULTS AND ANALYSIS

A. Calculation of susceptibility

The dynamical susceptibility $\chi''(\nu)$ is given by

$$\chi''(\nu)=K(\nu_i-\nu)^{-4}[n(\nu)+1]^{-1}I(\nu), \tag{1}$$

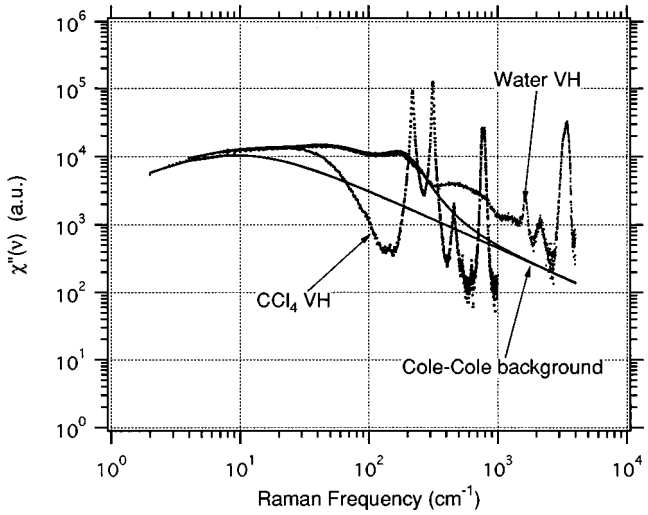

FIG. 1. Raman spectra of water and CCl_4 at room temperature. The solid line shows the fitted curve for water.

where $I(\nu)$ is the Raman spectral intensity, $n(\nu)=[\exp(hc\nu/kT)-1]^{-1}$ is the Bose-Einstein factor, ν_i is the frequency of incident laser light in cm^{-1}, K is the instrumental constant, T is the absolute temperature, and c is the velocity of light. The variable ν is the Raman frequency shift, also in cm^{-1}.

B. Difference between water and CCl_4 spectra

Figure 1 shows the $\chi''(\nu)$ spectra of CCl_4, water, and fitted result for water. Below 20 cm^{-1}, both CCl_4 and water have relaxational profiles. The fitting functions for water in the low-frequency region are composed of three components: Cole-Cole type relaxation and two damped harmonic oscillators. In the frequency range up to 4000 cm^{-1}, $\chi''(\nu)$ of water is larger than the high frequency tail of the Cole-Cole function due to the high background. On the other hand, the lowest relaxational component of CCl_4 decreases quickly above 20 cm^{-1} and the spectral profile becomes lower than the high frequency tail of the Cole-Cole function. Therefore the Cole-Cole function cannot be applied to the spectral fitting of $\chi''(\nu)$ in CCl_4.

C. Multiple random telegraph (MRT) model (Ref. 10)

Debye-type dielectric relaxation is useful for relating the molecular dynamics to dielectric absorption and dispersion. It is well known that Debye relaxation breaks down in the high frequency region ($\sim$1 THz, i.e., $\sim$30 cm^{-1}) because of inertia and memory effects. Debyes theory of rotational diffusion produces a plateau in the far infrared power absorption. Therefore several authors have proposed various theories of dielectric relaxation taking into account the inertia and memory effects.[11,12] Shibata *et al.* have developed an exactly solvable model incorporating inertia and memory effects using multiple random telegraph processes. The model is quite general and accounts for many existing models as special cases, and has a simple form making it suitable for practical applications. Bagchi and Chandra have developed another solvable model for dielectric relaxation,[13] but their model is too complicated to use for fitting analysis. In the present paper we use the imaginary part of the dielectric relaxation, calculated from Shibata's MRT model, to fit the reduced Raman spectra.

The complex dielectric spectrum has the form

$$\chi^*(\omega)=1-i\omega v[s], \tag{2}$$

where $s=i\omega$.

In asymmetric case, $v[s]$ is given by the continued fraction,

$$v[s]=\cfrac{1}{s+\cfrac{N\tilde{\Delta}_0^2}{s+\tilde{\gamma}+\cfrac{2(N-1)\tilde{\Delta}_0^2}{s+2\tilde{\gamma}+\cfrac{3(N-2)\tilde{\Delta}_0^2}{s+3\tilde{\gamma}+\cdots}}}}\Bigg/\cfrac{N\tilde{\Delta}_0^2}{s+(N-1)\tilde{\gamma}+\cfrac{N\tilde{\Delta}_0^2}{s+N\tilde{\gamma}}} \tag{3}$$

where $\tilde{\Delta}_0{}^2=\Delta_0{}^2(1-\sigma^2)$ and $\tilde{\gamma}=\gamma-2i\sigma$. The multiple random telegraph process is composed of N independent random telegraph processes that take the value $\pm\Delta_0$. γ is the inverse of the characteristic time of the random telegraph process. Nonzero values of σ mean that each probability of the random telegraph processes is asymmetric. We use Δ_0, $\alpha_0(=\Delta_0/\gamma)$, σ, N and the relaxation strength as fitting parameters and the Levenberg-Marquardt method is used to obtain a best fitted result. This algorithm changes each parameter during estimation, but N must be a positive integer. Thus we select a value of N and fit the other parameters using the nonlinear least square method. We try typical N values such as 1, 2, 5, 10, 20 and 50. This model contains two specific cases: the Gaussian-Markovian limit ($N\to\infty$) and the narrowing limit ($\alpha_0\ll 1$; corresponding to Debye-type relaxation).

In the time domain, $v(t)$, the inverse Laplace transform of $v[s]$ has the form

$$v(t)=\{\cosh(\tilde{\gamma}t/2\tilde{a})+\tilde{a}\,\sinh(\tilde{\gamma}t/2\tilde{a})\}^N e^{-N\tilde{\gamma}t/2}, \tag{4}$$

where

$$\tilde{a}=[1-4(\tilde{\Delta}_0/\tilde{\gamma})^2]^{-1/2} \tag{5}$$

and $v(0)=1$. $v(t)$ is the time correlation function of the dielectric function. In the case of our fitting results, $|v(t)|$ decreases monotonically and becomes an envelope line for the real and imaginary parts of $v(t)$ (Figs. 5(a), 5(b)). Therefore we define the characteristic relaxation time τ as the solution of the following equation

$$|v(t)|-\tfrac{1}{2}=0. \tag{6}$$

We put the value of ω (in cm^{-1}) into Eq. (3) to obtain the fitting parameters. This procedure is justified because this model uses scaled parameters. Therefore both ω and τ have no dimension. The relaxation time τ_n (no dimension) in the frequency (cm^{-1}) domain is calculated from Eq. (6) with the

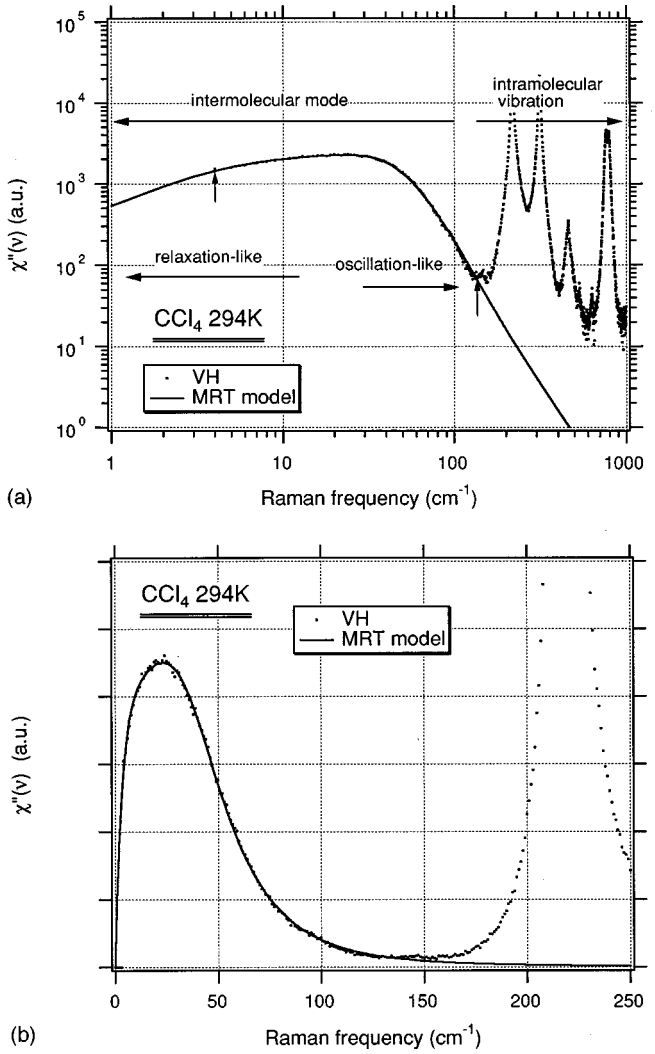

FIG. 2. (a) Depolarized Raman spectrum of CCl_4 (dotted line). Intermolecular mode appeared below 100 cm^{-1}. Below 20 cm^{-1}, this broad peak is relaxation-like. From 30 cm^{-1} to 100 cm^{-1}, this mode is oscillation-like and its intensity decreases rapidly. The best fitted result using the imaginary part of the MRT model is shown by the solid line. Vertical arrows show the fitted region of the spectrum. (b) Low-frequency part of (a).

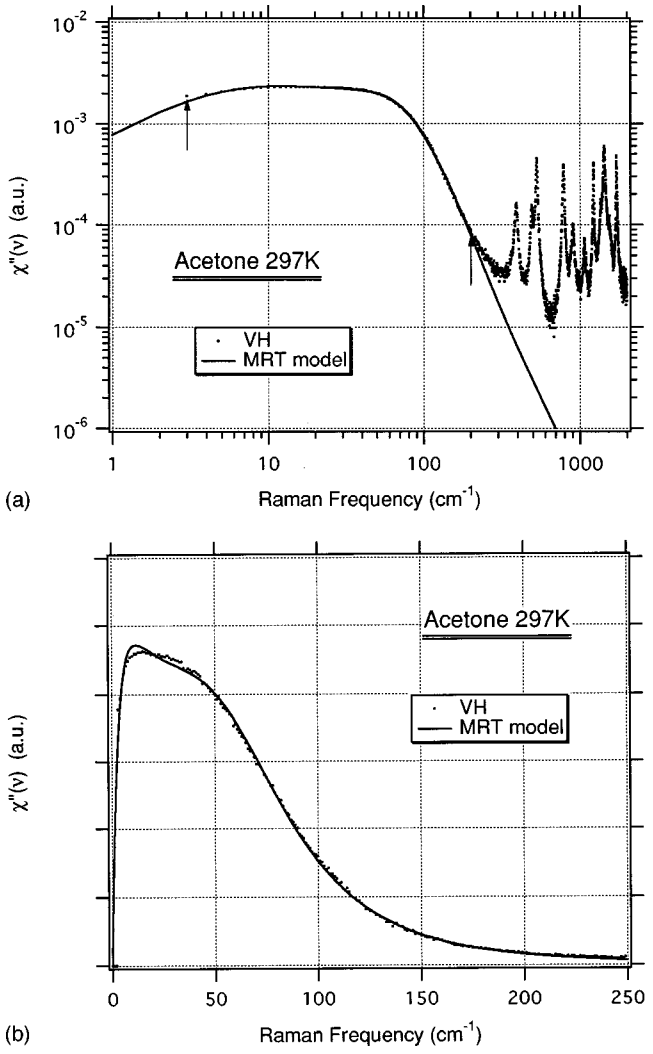

FIG. 3. (a) Depolarized Raman spectrum of acetone at room temperature (dotted line). The best fitted result using the imaginary part of the MRT model is shown by the solid line. Vertical arrows show the fitted region of the spectrum. (b) Low-frequency part of (a).

fitting parameters. Finally, we divide τ_n by the scaling factor $2.99\times10^{10}\times2\times\pi$ to obtain the relaxation time in seconds.

D. Fitting results

Figure 2(a) shows the reduced Raman spectrum of CCl_4 and the fitted result in a log-log plot. The vertical arrows shows the starting and end points of the fitting region. Below 100 cm^{-1}, there is a broad peak due to intermolecular motion. The low frequency part of this mode resembles relaxation, but the high frequency tail decreases like oscillation. Neither Debye-type relaxation nor damped oscillator models can fit this type of spectrum. The MRT model can fit this spectral feature well. Figure 2(b) shows a log-linear plot of the low-frequency Raman spectrum of CCl_4 and the fitted curve.

Figures 3(a) and 3(b) show the reduced Raman spectrum of acetone with the fitted result. Above 50 cm^{-1}, the spectral profile decreases more rapidly than that of Debye-type relaxation. The present MRT model can fit this spectral profile of acetone well.

Figures 4(a) and 4(b) show the reduced Raman spectrum of chloroform ($CHCl_3$). Above 80 cm^{-1} the spectral profile of chloroform decreases more quickly than that of the MRT model. This feature becomes more obvious as the fitted curve deviates from the spectrum above 100 cm^{-1}.

Figures 5(a) and 5(b) show $v(t)$ calculated from fitting parameters of CCl_4. $v(t)$ is a complex function and we denote $v^*(t)=v'(t)+iv''(t)$. The absolute value of $v^*(t)$ monotonically decreases and becomes an envelope line of both the real and imaginary parts of $v(t)$. From Eq. (6) we can obtain the relaxation time. Table I shows the best fitted result and relaxation time for each liquid.

IV. DISCUSSION

The dielectric function is written in the form

$$\frac{\varepsilon^*(\omega)-\varepsilon_\infty}{\varepsilon_s-\varepsilon_\infty}=1-i\omega\int_0^\infty dt e^{-i\omega t}\hat{\psi}(t), \tag{7}$$

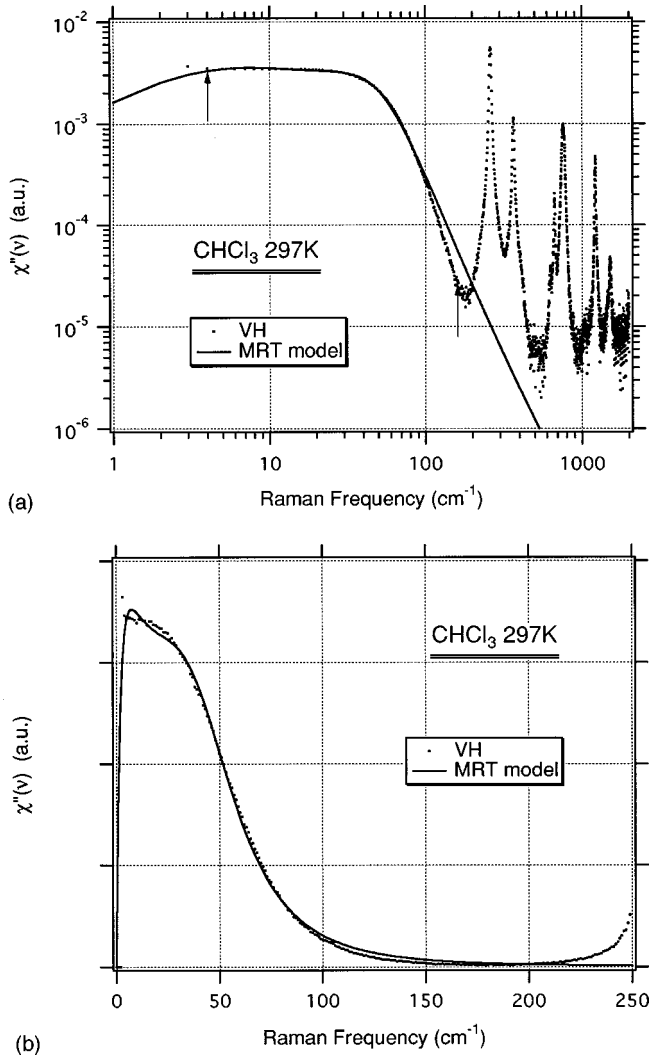

FIG. 4. (a) Depolarized Raman spectrum of chloroform at room temperature (dotted line). The best fitted result with the imaginary part of the MRT model is shown by the solid line. Vertical arrows show the fitted region of the spectrum. Above 100 cm^{-1}, susceptibility decreases faster than the fitted result. (b) Low-frequency part of (a).

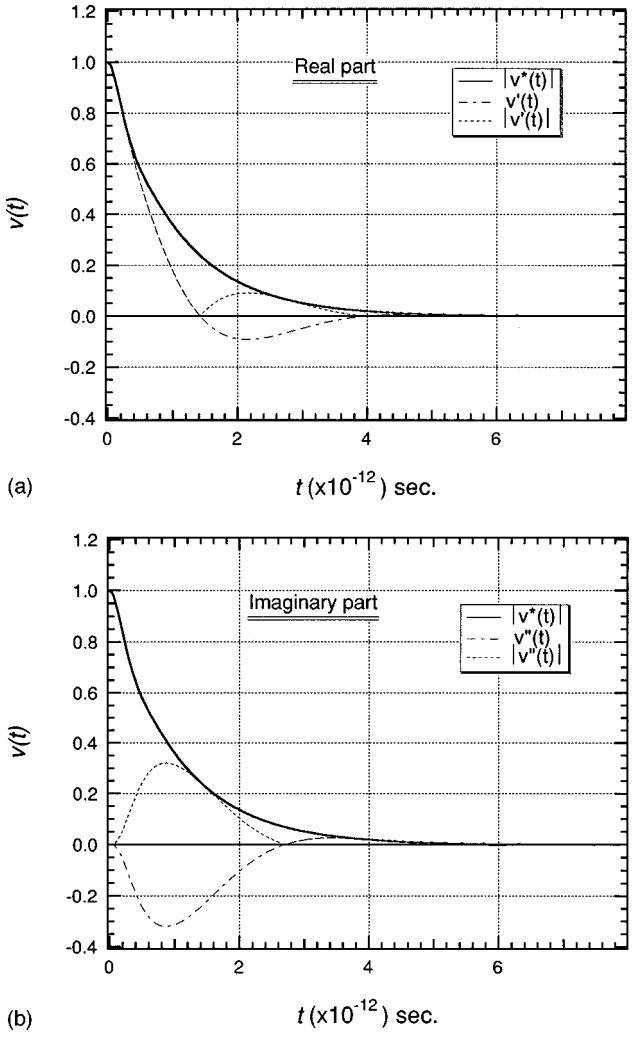

FIG. 5. $v(t)$ calculated using the best fit parameters of CCl_4. (a) Real part of $v(t)$ with its absolute value. Solid line shows the norm of the complex value $|v^*(t)|$, dotted and dashed-dotted lines show the real part of $v(t)$ and its absolute value $|v'(t)|$, respectively. (b) Imaginary part of $v(t)$ with its absolute value. Solid line shows the norm of the complex value $|v^*(t)|$, dashed-dotted line shows the imaginary part of $v''(t)$ and the dotted-line shows its absolute value.

where

$$\hat{\psi}(t)=\frac{\beta}{\psi(0)}\langle\mu(t);\mu(0)\rangle \tag{8}$$

is a relaxation function ($\beta=1/k_BT$, T is the absolute temperature and μ represents the electric dipole moment). On the other hand, the complex susceptibility

$$\chi_{ll'}(\omega)=\int_0^\infty dt e^{-i\omega t}\phi_{ll'}(t) \tag{9}$$

is represented by the oscillator correlation function

$$\phi_{ll'}(\omega)=-\langle[q_l(t),q_{l'}(0)]\rangle, \tag{10}$$

where [ ] are Poisson brackets. q_l is the lth mode of molecular motion, typically intramolecular vibration. We suppose that q_l is not necessarily vibrational motion. Any motion which can modulate polarizability is a candidate for the origin of Raman susceptibility. Rotational Brownian motion or other types of diffusional motion will produce Raman intensity in the low-frequency region. We suppose that the same kind of stochastic process underlies Eqs. (8) and (10). Abdrakhamanov *et al.* have already shown the equivalence between the reduced light scattering spectrum and the far infrared absorption spectrum.[14] We apply the calculated response based on Eqs. (7) and (8) to reduced Raman spectra.

TABLE I. Fitting parameters.

	CCl_4	$CHCl_3$	Acetone
Intensity (a.u.)	6979.2	0.018767	0.01047
Δ_0	21.7574	22.525	30.674
α_0	0.684885	0.68718	0.66185
σ	0.766723	0.86719	0.9939
n	2	2	50
$\tau(10^{-12}$ sec.)	0.6565493	1.198276	0.7872546

Recently Flanders *et al.* reported the frequency dependent absorption spectra of CCl_4 and $CHCl_3$ as measured by THz time domain transmission spectroscopy.[6] Figure 8 in Ref. 6 shows their experimental data for $CHCl_3$ and CCl_4. The CCl_4 spectrum has a profile similar to our results. $\alpha''(\omega)$ of CCl_4 in the low frequency region increases smoothly, while that of $CHCl_3$ increases sharply and changes shape at 0.5 THz. In our results, $\chi''(\nu)$ of CCl_4 increases smoothly then gradually decreases, but the initial increase in $\chi''(\nu)$ of $CHCl_3$ cannot be observed due to the resolution limit of spectrometer.

Mori's third-order continued fraction, which is used for analysis in Ref. 6, provides a Debye relaxation time $\tau_D = 6.36$ ps and a longitudinal relaxation time $\tau_L = 3.13$ ps. In our results, the characteristic relaxation times of CCl_4 and $CHCl_3$ are 0.66 ps and 1.20 ps, respectively. The positions of peaks in the spectra are substantially the same, 1.1 THz in Ref. 6 and 30 cm^{-1} ($\approx$1 THz) in our results. Thus, around 30 cm^{-1} both modes have the same origin; a certain type of molecular dynamics, and the difference in the relaxation times depends on the relaxation models adopted.

The number of parameters in Mori's continued fraction increases with the order of the continued fraction. In contrast to Moris' formula, Shibata's MRT model has only 5 parameters and the number of parameters does not depend on the order of the continued fraction. α_0 represents the modulation speed and is related to the correlation (memory effect) of the random noise. Nonzero values of σ indicate that the fluctuation has asymmetrical probability and N is the number of superposed random telegraph processes. These parameters are phenomenologically related to the microscopic structure of molecular liquids.

Although the MRT model reconstructs quantitatively the reduced Raman spectra of CCl_4 and acetone, the fitted result for $CHCl_3$ using the MRT model is only qualitative. The MRT curve decreases more slowly than the experimental result above 100 cm^{-1}. If we postulate that a Gaussian mode exists around 60 cm^{-1}, the fitting result is much improved because the strength of the MRT model can be reduced. The origin of the Gaussian mode is the subject of future work.

V. CONCLUDING REMARKS

Depolarized low-frequency Raman spectra of CCl_4, $CHCl_3$ and acetone were measured and analyzed using the MRT model of dielectric relaxation. Debye and Cole-Cole type relaxation functions cannot be applied to these spectra due to the difference between the intramolecular and intermolecular modes. The relaxational mechanism of intermolecular interactions is not entirely clear, but in the present paper we have shown that the equations of motion and the stochastic process of fluctuation would be similar to those of rotational Brownian motion. The overdamped limit and the narrowing limit approximations are appropriate only below about 30 cm^{-1} and break down above 30 cm^{-1}. Low-frequency Raman spectra exhibit the behavior similar to infrared absorption spectra.

ACKNOWLEDGMENTS

The authors would like to thank Professor F. Shibata for many discussions and helpful advice. This work is partly supported by a Grant-in-Aid for Scientific Research from the Ministry of Education, Science, Culture, and Sport.

[1] K. Mizoguchi, Y. Hori, and Y. Tominaga, J. Chem. Phys. **97**, 1961 (1992).
[2] Y. Wang and Y. Tominaga, J. Chem. Phys. **104**, 1 (1996).
[3] Y. Tominaga and S. M. Takeuchi, J. Chem. Phys. **104**, 7377 (1996).
[4] S. Palese, S. Mukamel, R. J. D. Miller, and W. T. Lotshaw, J. Phys. Chem. **100**, 10380 (1996).
[5] Y. J. Chang and E. W. Castner, Jr., J. Phys. Chem. **98**, 9712 (1994).
[6] B. N. Flanders, R. A. Cheville, D. Grischkowsky, and N. F. Scherer, J. Phys. Chem. **100**, 11824 (1996).
[7] S. R. Keiding, J. Phys. Chem. A **101**, 5250 (1997).
[8] J. T. Kindt and C. A. Schmuttenmaer, J. Phys. Chem. **100**, 10373 (1996).
[9] C. Rønne, L. Thrane, P.-O. Åstrand, A. Wallqvist, K. V. Mikkelsen, and S. R. Keiding, J. Chem. Phys. **107**, 5319 (1997).
[10] F. Shibata, C. Uchiyama, and K. Maruyama, Physica A **161**, 42 (1989).
[11] J. McConnell, *Rotational Brownian Motion and Dielectric Theory* (Academic, London, 1980).
[12] M. Evans, G. H. Evans, W. T. Coffey, and P. Grigolini, *Molecular Dynamics and Theory of Broad Band Spectroscopy* (Wiley, New York, 1982).
[13] B. Bagchi and A. Chandra, J. Chem. Phys. **93**, 1955 (1990).
[14] B. M. Abdrakhmanov, A. I. Burshtein, and S. I. Temkin, Chem. Phys. **143**, 297 (1990).